



2-D Waveform and Traveltime Inversion for Seismic Imaging, Naga Thrust Belt, India.

Priyank Jaiswal and Colin A. Zelt,*

Department of Earth Science, Rice University, 6100 Main Street, Houston, Texas – 77005, USA

Rahul Dasgupta, Oil India Limited, Duliajan, Assam, India

Summary

In the Assam region of northeast India, imaging of the Naga thrust fault suffers both from acquisition related noise and a limited understanding of the thrust-belt geology. In such an area the utility of 2-D traveltime and waveform inversion as supplements to conventional imaging and interpretation processes is demonstrated. First, a smooth velocity model with long wavelength characteristics of the subsurface is estimated through 2-D inversion of first arrival traveltimes. Next, the smooth velocity model is used for depth-migration and interpretation of the thrust fault. The quality of part of the migrated image that is poorly resolved due to processing limitations is enhanced using 2-D waveform inversion.

Introduction

Drilling for hydrocarbons in the Naga thrust belt in the Assam province has traditionally been guided by surface manifestations of the thrust. Towards the northeast, the thrust fault deepens leaving subtle surface expressions that are further obscured by thick vegetation. In such an area, wide-aperture 2-D seismic data were collected along a line approximately perpendicular to the trend of the thrust belt. The data have a moderate signal-to-noise ratio and suffer from ground roll and other acquisition related noise. Furthermore, lack of adequate understanding of the thrust-belt geology limits the ability of conventional processing to yield a reliable velocity model which in turn leads to a poor subsurface image. In this paper we demonstrate the utility of 2-D traveltime and waveform inversion in estimating a velocity model that can be used for both conventional processing and interpretation.

As a first step, a smooth velocity model with long wavelength characteristics of the subsurface is estimated through inversion of the first arrival traveltimes. Following traveltime inversion, the interpretation of the deeper (> 500 m) and shallower (< 500 m) portions of the thrust fault is achieved using the inverted velocity model and different methodologies. For the deeper interpretation of the fault, a Kirchoff pre-stack depth migration is performed. For interpretation of the fault in the shallow subsurface, where the quality of the depth-migrated image is poor, the resolution of the velocity model from traveltime inversion is enhanced by 2-D waveform inversion allowing direct interpretation of the geology. This study demonstrates that a combination of traveltime and waveform inversion with conventional processing is a promising approach for interpretation of geological structures in a thrust belt.

Geological Setting

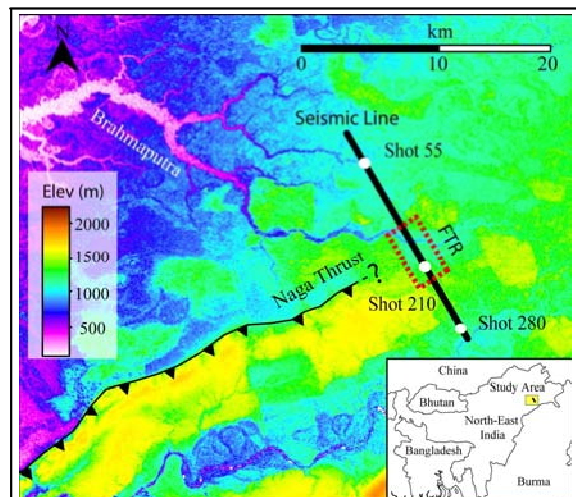


Figure 1. Acquisition layout and elevation map. Location of the study area with respect to northeast India is shown in inset. The layout of the seismic line is shown with a solid black line. The Naga thrust fault is interpreted after Dasgupta and Biswas (2000). Also labeled is the river Brahmaputra. Data from shots 55, 210 and 280 (solid white circles) are displayed in Fig. 2. The area between the dotted red lines is referred to as the fault trace region (FTR); see text for details. Northwest and southeast of the FTR are referred to as the foreland region (FR) and the thrust belt region (TBR) respectively.



"HYDERABAD 2008"

The geological structures under investigation in this study are part of a young fold and thrust belt that were formed as a result of collision between the Indian and Eurasian subcontinents in the mid-miocene. The foreland of this thrust belt is the alluvium plain of the river Brahmapurta (Fig. 1) and it is characterized by well stratified fluvial sediments, the Namsang formation, up to a depth of ~ 2 km. Drilling results from the vicinity of the study area reveal that the Naga thrust sheet comprises of three distinct geological units. On top is a flood plain clay rich unit of upper Miocene age known as the Girujan formation overlying a massive sand rich deltaic unit of mid-Miocene age known as the Tipam formation. The Tipam formation in turn overlies an upper Eocene - lower Oligocene Barail Group deposited in a marginal-marine to fluvial setting.

Seismic Acquisition and Data

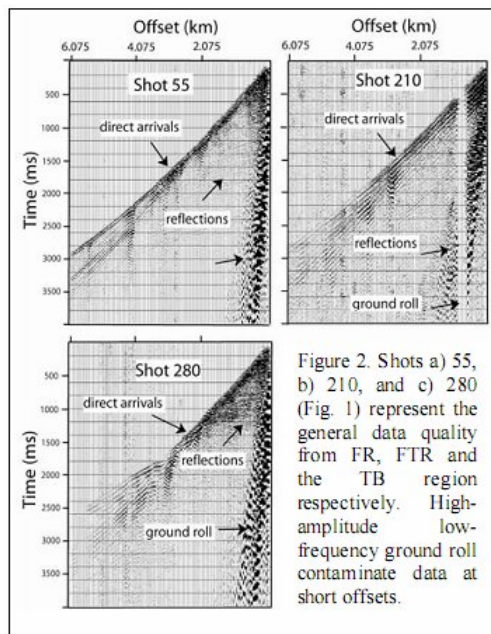


Figure 2. Shots a) 55, b) 210, and c) 280 (Fig. 1) represent the general data quality from FR, FTR and the TB region respectively. High-amplitude low-frequency ground roll contaminate data at short offsets.

The seismic line used in this study is ~20 km long with 50m shot and receiver spacing and a nominal fold of 60. The acquisition style is end-on. 313 shots with maximum offsets of ~6 km are fired by placing dynamite in boreholes 30 m deep. Representative shot gathers from the northeast, center, and southwest part of the line are displayed with true amplitudes in Fig. 2. Shot gathers from the central part of the line suffer from reverberations most likely due to trapped energy in the hanging wall of the thrust belt. In general the data quality deteriorates from northeast towards the southwest end of the line.

Traveltime Inversion

Inversion of the first arrival times is implemented using the regularized Zelt and Barton (1998) method. Data for traveltime inversion comprise ~6500 first arrival times from 67 shots spaced evenly ~300 m along the line. Uncertainties of 8 - 20 ms were assigned to the first arrival traveltimes picks based on dominant frequency and ambient noise. The starting model for traveltime inversion is constructed by

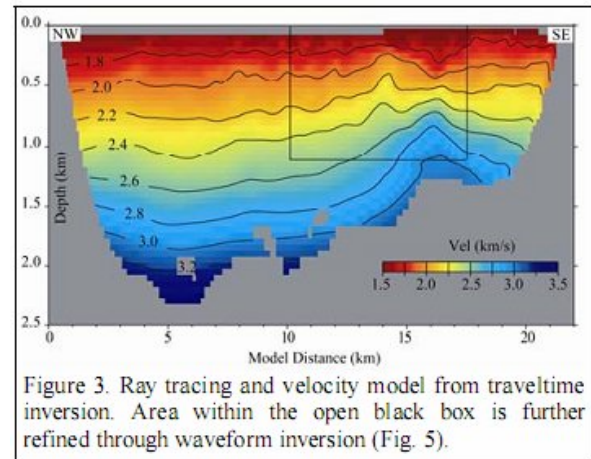


Figure 3. Ray tracing and velocity model from traveltime inversion. Area within the open black box is further refined through waveform inversion (Fig. 5).

averaging regional drilling results (personal communication, Oil India Ltd); it is laterally homogeneous and has a linearly increasing velocity function with depth (1.5 km/s at surface to 3.5 km/s at 2 km depth). The final model (Fig. 3) evolved from the flat layer-cake initial model and converged with a normalized data model (Fig. 3) evolved from the flat layer-cake initial model and converged with a normalized data misfit error close to unity in ten iterations.

Pre-Stack Depth Migration

Final velocity model from traveltime inversion is used for Kirchoff pre-stack depth migration of the near normal incident data. The migrated image using inverted velocities

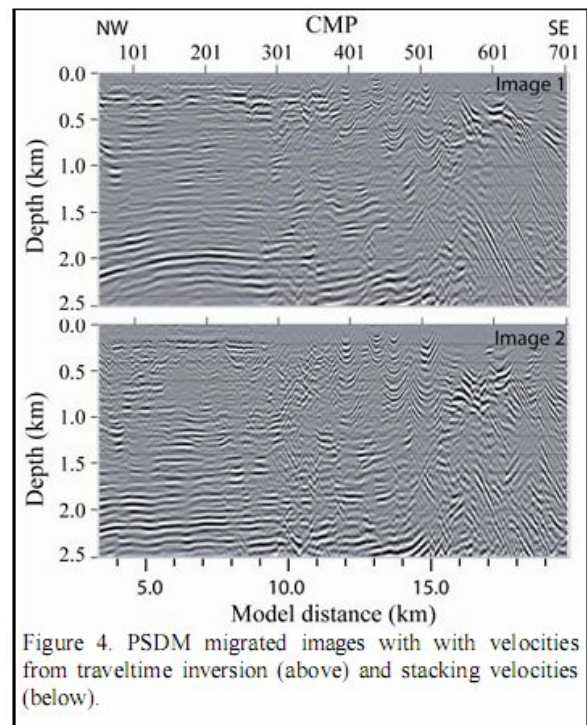


Figure 4. PSDM migrated images with with velocities from traveltime inversion (above) and stacking velocities (below).



"HYDERABAD 2008"

is compared to its counterpart using hand-picked stacking velocities (Fig. 4) for a preliminary appreciation of the traveltimes inversion result both in terms of its overall geological reasonability and ability to improve the depth migration. Overall Image 1 appears to have higher signal-to-noise ratio than Image 2. An anticlinal feature at a depth of ~2 km between CMPs 101 and 201 which is prominent in Image 1 is almost unidentifiable in Image 2. Reflection events in Image 1 compared to Image 2 are more focused and coherent. Compared to Image 2, the southeast dipping reflectors between CMPs 500 and 700 (representing the hanging wall of the naga thrust) are better identified in Image 1. In the central part of the line, where the Naga thrust fault is anticipated, the quality of the shallow (< 1km) migrated image is poor due to muting of the near offset data to avoid the effects of ground roll and ringing on migration. The shallow resolution is improved using waveform inversion described in the next section.

Waveform Inversion

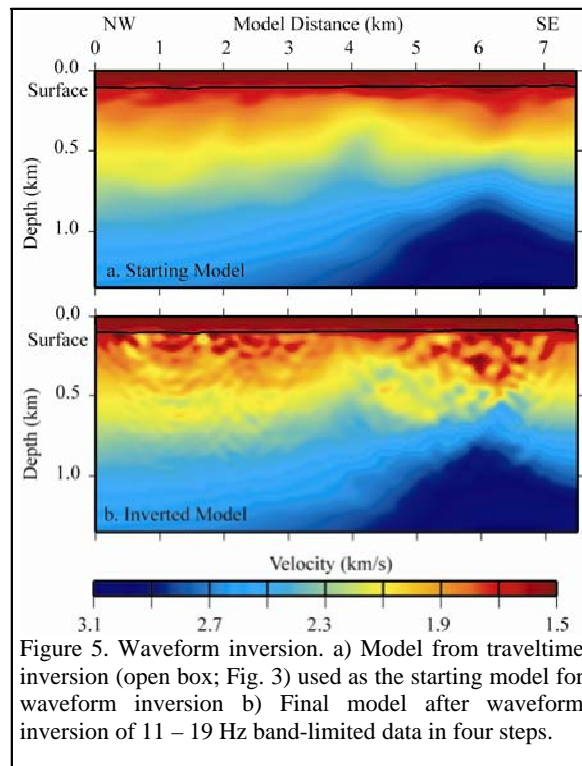


Figure 5. Waveform inversion. a) Model from traveltimes inversion (open box; Fig. 3) used as the starting model for waveform inversion b) Final model after waveform inversion of 11 – 19 Hz band-limited data in four steps.

The 2-D waveform inversion is implemented in frequency domain after Pratt (1999) using a multi-scale approach advocated by Bunks et al. (1995) to mitigate the non-linearity of the inverse problem.

The part of the velocity model from traveltimes inversion that is improved using waveform inversion is indicated by an open box in Fig. 3. The dataset used for waveform inversion comprises the coda close to the direct arrivals corresponding to ~5000 shot-receiver pairs obtained by windowing 88 shot gathers in offset (0.5 - 4.0 km) and time (1s from the first break picks). These data correspond to all shots that lie within the zone of interest (open box, Fig. 3). The window is applied to ensure a high signal-to-noise ratio and exclusion of features such as ringing, ground rolls, and mode-converted later arrivals that are beyond the realm of the acoustic wave approximation made in this study. Examination of the windowed data indicates 11 Hz to be the lowest usable frequency. A high cut filter of 25 Hz applied to the data limits the resolution of the inverted model to a length scale that is desired for interpretation in this study.

Waveform inversion began with determination of the source signature using the starting model (open box, Fig. 3) and the band limited real data. Following this, forward modeling with the starting model and the initial source signatures was performed to bulk scale the real shot gathers such that the variations of the root mean square amplitudes of individual traces with offsets of the real and synthetic shot gathers have the same mean.

The starting model (open box, Fig. 3; Fig. 5a) yielded the final model (Fig. 5b) successively in four steps. In each step a frequency bandwidth of 2 Hz were inverted simultaneously. First to fourth step corresponded to successive inversion of 11-13Hz, 13-15Hz, 15-17Hz, and 17-19Hz frequency bandwidths respectively. The inversion was halted at the end of fourth step when the resolution desired for interpretation was achieved. The updated model from each step was used as the starting model for the next step. Prior to updating the velocity model in each step, the source signature was re-calculated using the updated velocity model from the previous step. Successive incorporation of higher frequencies in every step yielded higher wavenumber solution of the geology. A series of checkerboard resolution tests of the starting model with band-limited real data and final source signature indicate that velocity anomalies with dimensions of at least 200 X 100 m (horizontal X vertical) and perturbations of 10% could be well recovered in the region where interpretation of the geological features are intended.

Interpretation

The northwest end of the traveltimes model, which is essentially 1-D in character (Fig. 3a), is indicative of the foreland basin. The shallow part (< 1.8 km/s velocity contour) of the model with rugged structure may be representative of the weathered layer. From the northwest



"HYDERABAD 2008"

end towards the center of the model the velocity contours hallow most likely due to the effect of the Naga thrust. The pull-up of high velocity at ~17 km suggests the presence of the Naga thrust fault. Towards the southeast end, high velocity (2.6 – 3.0 km/s) show a deepening most likely representing the hanging wall (Fig. 3a).

A composite of the migrated images and the perturbation model from waveform inversion facilitates interpretation of small-wavelength features (Fig. 6). The perturbation model in Fig. 6 is the difference between the initial and final waveform model presented in two colors where negative and positive perturbation with respect to the starting model is respectively represented by darker and lighter shades. The near-horizontal layer-cake reflections from the northwest end of the line to ~CMP 400 represent the foreland region. Around CMP 450 at a depth of ~1.35 km, a change in the dip of the stratigraphy suggests presence of the fault and is interpreted as the Naga thrust fault (Th; Fig.6). At 11km traveltime model distance a normal fault is interpreted (N; Fig. 6). The southeast dipping horizons between CMP 600 and 700 appear to be truncated by another group of southeast dipping strata with lesser dip. The horizon along which the truncation occurs is interpreted as the mid Miocene unconformity (E; Fig. 6). Between CMP 300 and 600 to depth of ~1.35 km, interpretation is not possible due to the poor quality of the migrated image and is furthered in this part with the help of the perturbation model from waveform inversion. Between CMP 450 and 500, the perturbation model shows a faint expression of a northwest dipping feature; it is interpreted as the edge of the hanging wall. The interpretation of the Naga thrust fault in the migrated image is continued in the waveform inversion model guided by the edge of the hanging wall (dotted black line; Fig. 6).

Conclusions

The key in this paper is development of a smooth velocity model by inversion of first arrival traveltimes that is representative of the large-scale subsurface structures; it provides an overall geological insight and serves as input for both depth migration and waveform inversion. Migration results suggest that velocities from traveltime inversion are better suited for depth-migration than stacking velocities (converted to interval velocities). Resolution of the geological features imaged by waveform inversion is suitable for interpretational purposes in this paper. A multi-scale frequency-domain implementation of the waveform inversion with a band limited seismic data requires a reliable starting model, which in this paper is constructed with the help of traveltime inversion. A composite of migrated image and waveform inversion model is used for interpretation. The interpretation could be reconciled with the regional observations suggesting that a combination of first-arrival traveltime and waveform inversion with pre-stack depth-migration can be a promising approach in interpretation of the thrust geology.

References

- Dasgupta, A. B. & Biswas, A. K., Eds., 2000. Geology of Assam, Bangalore, Geological Society of India.
- Zelt, C. A. & Barton, P. J., 1998. Three-dimensional seismic refraction tomography: A comparison of two methods applied to data from the Faeroe Basin, *Journal of Geophysical Research-Solid Earth*, 103, 7187-7210.
- Bunks, C., Salec, F. M., Zaleski, S. & Chavent, G., 1995. Multiscale Seismic Waveform Inversion, *Geophysics*, 60,1457-1473.
- Pratt, R. G., 1999. Seismic waveform inversion in the frequency domain, Part 1: Theory and verification in a physical scale model, *Geophysics*, 64, 888-901.

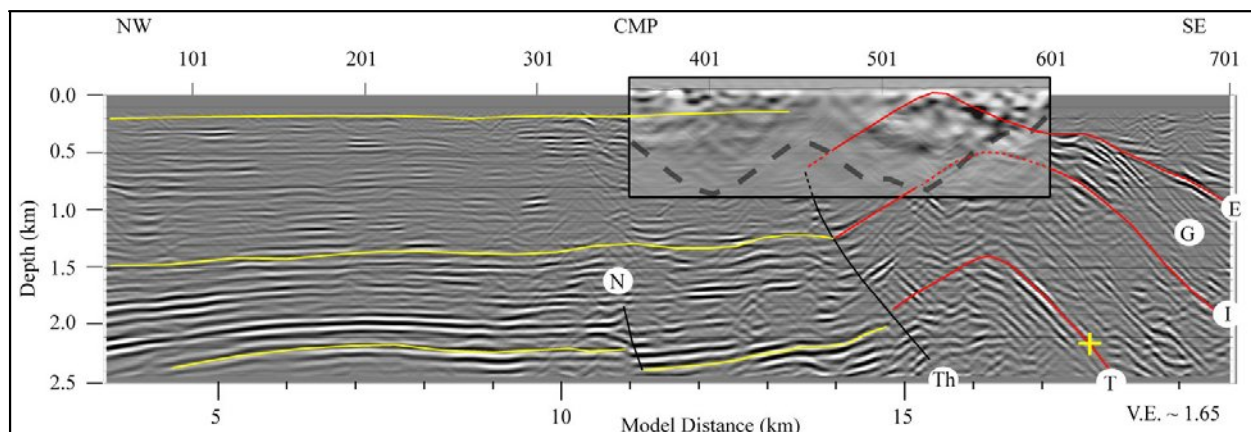


Figure 6. Composite interpretation. The features are labeled as follows: E - Miocene unconformity G - Girujan, I - sandy horizon within in the Gurujan, T - top Tipam, Th - Naga thrust fault, and N - normal fault. The foreland stratigraphy is interpreted with solid yellow lines. The yellow cross is a marker for a nearby exploratory well.